



ORIGINAL ARTICLE

Synthesis of highly stable MOF-5@MWCNTs nanocomposite with improved hydrophobic properties



Ata-ur-Rehman ^a, Syed Ahmad Tirmizi ^a, Amin Badshah ^a,
Hafiz Muhammad Ammad ^a, Muhammad Jawad ^b, Syed Mustansar Abbas ^{c,*},
Usman Ali Rana ^d, Salah Ud-Din Khan ^d

^a Department of Chemistry, Quaid-e-Azam University, Islamabad, Pakistan

^b Pakistan Institute of Engineering and Applied Sciences (PIEAS), Nilore, Islamabad, Pakistan

^c Department of Energy and Materials Engineering, Dongguk University, 30, Pildong-ro 1gil, Jung-gu, Seoul 100-715, Republic of Korea

^d Sustainable Energy Technologies (SET) Center, College of Engineering, King Saud University, PO-Box 800, Riyadh 11421, Saudi Arabia

Received 12 October 2016; accepted 24 January 2017

Available online 1 February 2017

KEYWORDS

Metal-organic frameworks (MOFs);
Carbon nanotubes;
Aspect ratio;
Nanocomposite;
Molecular statics simulations

Abstract Metal-organic frameworks (MOFs) are a promising class of nanoporous crystalline materials with potential applications in gas storage, catalysis, biomedical and clean energy. However, moisture adsorption dampens their structure and therefore capacity and selectivity. Improving the hydrostability of MOF-5 without compromising on its characteristic features can be a potential way to make the best use of this material. In this work, we used a solvothermal method to precipitate MOF-5 in well-dispersed carboxy derived MWCNTs. By inspiring from the hydrophobic properties of carbon nanotubes (CNTs), we have successfully utilized a solvothermal approach to precipitate MOF-5 in well-dispersed carboxy functionalized multiwalled carbon nanotubes (FMWCNTs) to produce a MOF-5@FMWCNTs nanocomposite. The experimental results in this study reveal that the FMWCNTs form stable nanocomposite with MOF-5 particles and the resultant hybrid MOF-5@FMWCNTs nanocomposite indicated an increase in the moisture stability and even after prolonged exposure to ambient moist environment (55% humidity at 28 °C) showed less degradation as confirmed by the BET surface area, and powder XRD studies. So, our findings

* Corresponding author.

E-mail address: qau_abbas@yahoo.com (S.M. Abbas).

Peer review under responsibility of King Saud University.



Production and hosting by Elsevier

demonstrate a simple synthetic route to make use of FMWCNTs to stabilize the MOF-5 and it can be a choice for many other MOFs without much compromise on the surface area.

© 2017 The Authors. Production and hosting by Elsevier B.V. on behalf of King Saud University. This is an open access article under the CC BY-NC-ND license (<http://creativecommons.org/licenses/by-nc-nd/4.0/>).

1. Introduction

Metal-organic frameworks (MOFs) have been seen as one of the most widely studied class of ordered porous solids (Bennett et al., 2016; Cui et al., 2016; Zhang et al., 2016). MOF structure is composed of metal-oxide units connected by organic linkages through strong covalent bonds that often have an extensive open-framework structure and enclosure of guest (usually solvent) can also take place during synthesis (Yang et al., 2014). To date, a wide range of metal ions and organic linkers have been utilized to design thousands of MOFs with a variety of topologies (Yue et al., 2015a, 2015b; Mihaly et al., 2016). The intense interest gained by these materials is rendered to their unsurpassed surface area and pore volume, which makes them a promising media for adsorption, storage and purification of gases, gas-sensing, biomedical imaging, drug delivery, secondary batteries, optical sensing, photovoltaics and other catalytic applications (Zhao et al., 2016; Zou et al., 2016). Recently many groups reported MOFs conversion on calcination into different carbonaceous materials such as carbon nanotubes, nanorods and graphene (Liu et al., 2008; Hu et al., 2012; Tang and Yamauchi, 2016). MOFs can also serve as light-weight molecular selective sieves, because of their extremely high surface areas and very narrow pore size distributions (Li et al., 1999; Yaghi et al., 2003; Kitagawa et al., 2004; Rowsell and Yaghi, 2004; Férey et al., 2005; Saha et al., 2009; Wei et al., 2013).

Different strategies have been opted to enhance framework structural stability of MOFs (Zhang et al., 2014). Gadipelli et al showed that postsynthetic thermal annealing at different temperatures affects MOFs structure and can enhance their gas sorption properties (Gadipelli and Guo, 2014). Recently, some attempts have been made to introduce polymer units to stabilize water sensitive MOFs (Ding et al., 2016; Gamage et al., 2016). Another way to boost up the water resistant properties is to dope with various metals and nonmetals. Li et al. have reported that Ni-MOF-5 showed increased water resistance and their MOF-5 framework starts decomposing after two days but still showed some MOF-5 peaks after a week at a relative humidity of 30–37% (Li et al., 2012). Carbon-based materials and nanoparticle loading efforts for hydrostability of MOFs have also been utilized, and Kim et al. have used carbon black and platinum nanoparticles (CB/Pt/MOF-5) to increase hydrogen storage capacity and hydrostability of their CB/Pt/MOF-5 composite (Kim et al., 2015). Recently, MOF-derived carbons have been proposed for electrochemical applications and once the MOFs are converted to pure carbon, the structural stability is increased (Torad et al., 2013; Tang et al., 2015; Tang and Yamauchi, 2016). Nguyen et al. have investigated post-synthetic modification (PSM) for various MOFs and reported superhydrophobicity by post-synthetic tailoring with alkyl and amide groups (Nguyen and Cohen, 2010). Yang et al used MOF-CNTs composites with high surface area and reported MOF-5 crystal reflections after exposure to a 33% relative humid environment (Yang et al., 2009).

MOF-5 [Zn₄O(BDC)₃; BDC = 1,4-benzenedicarboxylate] is one of the most promising and well-studied MOF (Rosi et al., 2003). It consists of tetrahedral Zn₄O units connected by linear 1,4-benzenedicarboxylate struts to form a cubic network structure. MOF-5 has been chosen for the present study because MOF-5 is quite thermostable, shows high porosity and has a high adsorption capacity for CO₂ and H₂, suggesting it to be a promising gas storage medium. However, like other MOFs, MOF-5 is extremely water-sensitive and it shows a sharp reduction in structural stability, gas adsorption capacity and surface area after exposure to humid air (Kaye et al., 2007; Tsao et al., 2007; Han et al., 2008; Zhao et al., 2009). Enhanced hydrostabil-

ity, molecular recognition, signal transduction and gas adsorption properties make metal loaded MOFs and MOF nanocomposites very useful materials for several device applications (Burtch et al., 2014; Wang et al., 2015; Yue et al., 2015a, 2015b). As a matter of fact, carbon nanotubes (CNTs) are known to have a hydrophobic nature (Lu et al., 2009; Pasiaka et al., 2014). By functionalizing CNTs, the properties can be tailored further and therefore, functionalized multiwalled carbon nanotubes (FMWCNTs) even show improved dispersion in different media (Sheikholeslam et al., 2012; Chang et al., 2015). It has been reported that the MOF-5@FMWCNTs nanocomposite has much higher structural stability, surface area and H₂ storage capacity (Yang et al., 2009; Petit et al., 2011; Li et al., 2012; Dai et al., 2013; Kang et al., 2015; Kim et al., 2015; Petit and Bandosz, 2015a, 2015b).

The present attempt has been made to further explore the affinity of FMWCNTs for MOF-5 particles, we have used a simple and unique synthetic strategy to see the nature of the interaction between FMWCNTs and MOF-5 particles. Our results reveal that the FMWCNTs develop mostly hydrogen bonding interactions with MOF-5 in MOF-5@FMWCNTs nanocomposite that plays a major role in the formation of stable nanocomposite material with improved adsorption capacity and retention of MOF framework along with enhanced surface properties as compared to water sensitivity of MOF-5 framework reported earlier (Yang et al., 2009).

2. Experimental

2.1. Materials

A.R. grade terephthalic acid, zinc nitrate hexahydrate (Zn(NO₃)₂·6H₂O), sulfuric acid, nitric acid and chloroform (CHCl₃, HPLC grade) were obtained from Merck, Germany. Diethyl formamide (DEF) and ethanol (anhydrous grade) were obtained from Sigma-Aldrich, Germany, whereas triethylamine (TEA) and hydrogen peroxide (H₂O₂) were purchased from RDH, Germany. In addition, cellulose nitrate membrane filters (0.22 μm) were obtained from Sartorius Stedim, Biotech, Germany, and MWCNTs were obtained from China. All the chemicals were used as received without any further purification.

2.2. Functionalization of MWCNTs

Functionalization of MWCNTs was carried out by a previously reported method adapted from the literature (Rehman et al., 2013). At first, 200 mg of MWCNTs were oxidized in air at 400 °C for 30 min to remove any amorphous carbon and adsorbed species present in the material. In order to remove the metal catalyst impurities, which have been incorporated into the MWCNTs during the synthesis process, MWCNTs were sonicated and refluxed in 3 M HCl at 70 °C for 3 h. These purified MWCNTs were sonicated and refluxed with a 100 ml mixture of 5 M HNO₃ and 30% H₂O₂ (1:1) for 8 h. Finally, the MWCNTs were filtered by cellulose nitrate membrane and washed with deionized water up to neutral pH. The resulting FMWCNTs showed an increased dispersion in DMF and DEF.

2.3. Synthesis of MOF-5 and MOF-5@FMWCNTs

The synthesis of MOF-5 was carried out by following the previously reported procedures with slight modifications such as using DEF as solvent (Tranchemontagne et al., 2008; Khan and Jhung, 2009; Lu et al., 2010). In brief, 15.2 mM of terephthalic acid was dissolved in 200 ml of DEF, followed by the addition of 3 ml of TEA into this solution mixture. Similarly, 30.0 mM of $\text{Zn}(\text{NO}_3)_2 \cdot 6\text{H}_2\text{O}$ was dissolved in 200 ml of DEF. The zinc solution was dropwise added to the terephthalic acid solution under sonication at 60 °C, resulting in white precipitates. The mixture was poured in glass vials, which were capped tightly and irradiated in a commercial microwave oven for 30 min. The precipitates were filtered and washed with 300 ml of DEF and immersed in CHCl_3 . The solvent was exchanged daily for 3 days. The product was filtered and dried under vacuum overnight at 120 °C. Similarly, MOF-5@FMWCNTs nanocomposite was synthesized by adding 5 wt.% of FMWCNTs to the above terephthalic acid solution, followed by sonication and dropwise addition of zinc solution and later for microwave treatment for 30 min as above for MOF-5. The nanocomposite sample was filtered, washed and dried in the same way as done for the MOF-5 earlier.

2.4. Sample characterization

Powder X-ray diffraction (XRD) measurements were undertaken using PANalytical X'pert PRO MRD XL. For Fourier transform infrared (FT-IR) spectroscopy, Thermo Scientific Nicolet-6700 spectrometer was utilized. Surface area and pore size analysis were made from Quantachrome, USA, NOVA200e using nitrogen adsorption measurements at liquid nitrogen temperature (77 K) and samples were degassed at 110 °C for 12 h to remove any entrapped guest molecules. For surface morphology studies, JEOL, JSM5910 for scanning electron microscope (SEM) and EFI-Titans for transmission electron microscope (TEM) were used. All samples were first dispersed in ethanol, sonicated in an ultrasonic bath, followed by dropwise loading of supernatant suspension onto a carbon coated copper TEM grid for analysis.

3. Results and discussion

Fig. 1 displays the XRD patterns for raw and HCl treated MWCNTs. The diffraction peaks centered at (ca.) 2θ values of 24.6° (002) and 42.4° (100) in the diffraction pattern of MWCNTs can be attributed to the hexagonal graphite structures. The sharpness of the peaks implies that the amorphous carbon content was significantly less, which is in accordance with the results obtained from SEM and TEM techniques, as described later. In particular, the diffraction peak ca. 24.6° 2θ in the XRD pattern of HCl purified MWCNTs was more sharp and intense, indicating a more ordered graphitic network of sp^2 -hybridized carbon atoms in this material (Yang et al., 2008).

The XRD patterns for MOF-5 (synthesized by microwave technique), MOF-5@FMWCNTs (as synthesized) and MOF-5@FMWCNTs (exposed to the ambient environment for one week) are shown in Fig. 2. All the samples can be indexed to cubic phase with a space group of $Fm\bar{3}m$ having $a = 25.7023 \text{ \AA}$ and $V = 16949.3 \text{ \AA}^3$. The XRD pattern matches

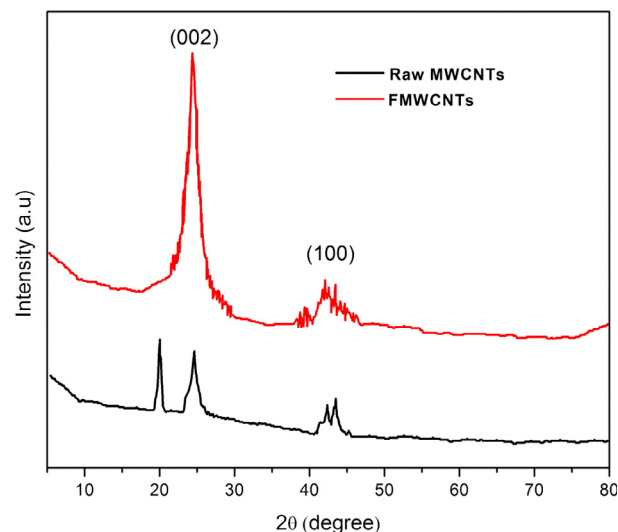


Fig. 1 XRD pattern of raw and functionalized MWCNTs.

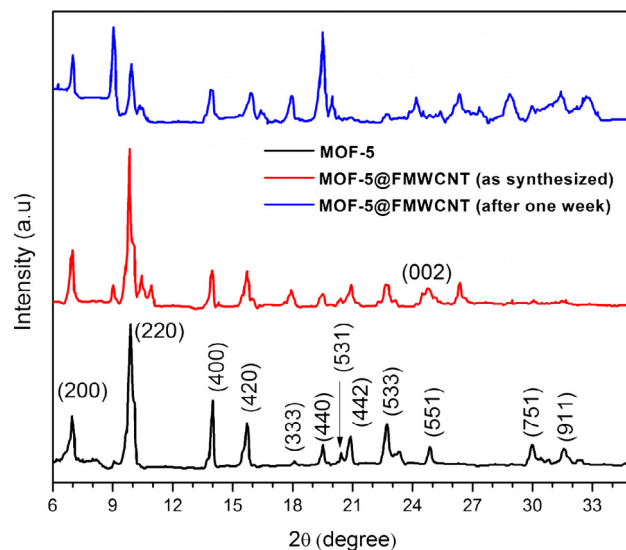


Fig. 2 XRD of MOF-5, MOF-5@FMWCNTs (as synthesized) and MOF-5@FMWCNTs (after one week).

with the MOF-5 pattern derived from single crystal structure data (Li et al., 1999). The main diffraction peaks ca. 6.9° 2θ and 9.8° 2θ confirm the successful synthesis of MOF-5 crystalline phases. Another characteristic peak ca. 24.8° 2θ representing MOF-5 crystalline plane was present in both MOF-5 and MOF-5@FMWCNTs nanocomposite, indicating the retention of the MOF-5 crystalline phases after the formation of the nanocomposite. However, the intensities of the two peaks at 6.9° 2θ and 9.8° 2θ were overturned that can be attributed to some alterations of atomic orientations in the crystal planes by adsorbed species (solvent and water molecules), unreacted zinc centers and framework interpenetration. The framework interpenetration also makes sense due to the presence of peak at 13.8° 2θ along with some unidentified peaks, which do not belong to MOF-5 crystal planes, suggesting the presence of an unidentified framework along with MOF-5

(Huang et al., 2003; Panella and Hirscher, 2005; Hafizovic et al., 2007; Kaye et al., 2007; Saha et al., 2009). The splitting of the peak at $9.8^\circ 2\theta$ is also an indication of the distortion in the cubic symmetry. A small peak appearing at $8.9^\circ 2\theta$ indicates that the decomposition of the MOF-5 structure is less intense in freshly prepared MOF-5 and MOF-5@FMWCNTs nanocomposite but increases in case of MOF-5 and MOF-5@FMWCNTs nanocomposite exposed to moist air conditions for one week. In addition, the ratio of the two peaks at $6.9^\circ 2\theta$ to $9.8^\circ 2\theta$ is also an indicator for the surface area of the MOF-5 and MOF-5@FMWCNTs nanocomposite.

From Fig. 3, the comparison of the FT-IR traces for the raw and FMWCNTs confirms the functionalization of MWCNTs after the acid treatment. The small difference of charge states on the highly symmetrical carbon atoms of the MWCNTs gives rise to a very small induced electric dipole, resulting in a silent spectrum and C=C peak at around 1600 cm^{-1} that are normally absent in the spectrum of raw MWCNTs. When MWCNTs are subjected to acid treatment, the high symmetry of MWCNTs is altered and induced electric dipoles are generated and infrared signals of C=C can be detected. The FT-IR spectrum of the functionalized MWCNTs displayed characteristic bands at 3641.6 cm^{-1} (corresponded to O—H stretching), 2976.6 and 2878.1 cm^{-1} (assigned to CH_2 stretching), 1748.5 cm^{-1} (assigned to C=O stretching of the carbonyl groups), 1606.3 cm^{-1} (corresponded to conjugated C=C stretching), 1361.3 cm^{-1} (associated with O—H bending deformation in —COOH) and $1300\text{--}1000\text{ cm}^{-1}$ (may be assigned to C—O stretch in carboxylic acid or alcohols).

The FT-IR spectrum of MOF-5 displayed two absorption bands ca. 2948.2 and 2870.7 cm^{-1} , which were assigned to C—H stretching vibrations of the methylene group. The vibration bands appearing at $1700\text{--}1400\text{ cm}^{-1}$ are assigned to the carboxylic functionality of the 1,4-benzenedicarboxylate. The strong peak appeared at 1758.1 cm^{-1} can be attributed to C=O stretching vibration of the carboxylate group of MOF-5. The contribution from the carbonyl CO bonds from the entrapped DEF solvent might also have contributed to this

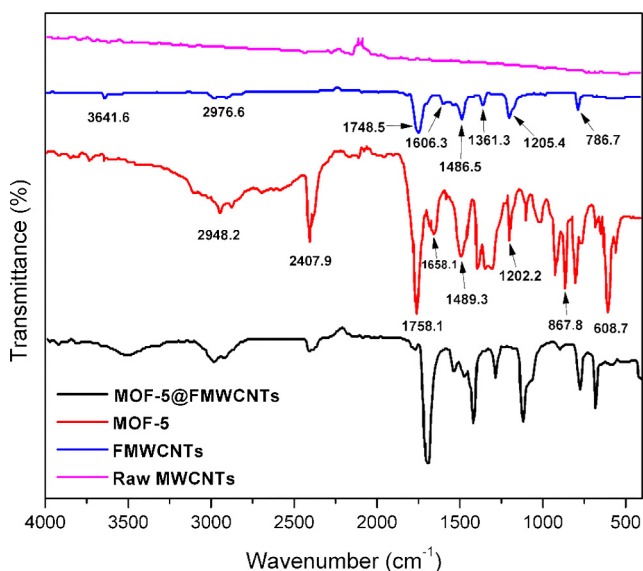


Fig. 3 FT-IR spectra of (a) raw MWCNTs, (b) functionalized MWCNTs, (c) MOF-5, and (d) MOF-5@MWCNTs.

peak. The carboxylate stretching peaks are likely to be decomposed into several components, having asymmetric vibration components displaying peaks at 1658.1 , 1583.3 , 1540.4 and 1489.3 cm^{-1} , while the symmetric stretching vibration appears at 1395.7 cm^{-1} . The symmetric stretching vibration of Zn_4O appearing at 608.7 cm^{-1} is also consistent with that of the literature (Bordiga et al., 2005; Greathouse and Allendorf, 2006; Sabouni et al., 2010).

In FT-IR spectrum of MOF-5@FMWCNTs, the majority of peaks for MOF-5 and FMWCNTs are retained. The appearance of a new broad vibration band $\sim 3550\text{--}3250\text{ cm}^{-1}$, which is not found in both MOF-5 and FMWCNTs, can possibly be linked to the formation of a hydrogen bond between O-atom of carboxylate moiety or ZnO_4 subunit of the MOF-5 framework and the H-atom of the —COOH functionality in FMWCNTs. This assumption is also supported by TEM results.

In the SEM image of MOF-5 (Fig. 4), uniformly sized cubic crystals are clearly evident. It is seen that the crystal sizes were smaller and well-structured than MOF-5 synthesized by other methods.

Fig. 5A displays the TEM image of FMWCNTs that clearly indicates the functionalization of MWCNTs as a result of acid treatment of the nanotubes, which also leads to some degree of shortening of these nanotubes. In Fig. 5B, C it is evident that FMWCNTs have been efficiently loaded with the MOF-5 and these functionalized nanotubes also get clustered around MOF-5 particles, possibly due to the formation of hydrogen bonding between O-atom of MOF-5 and H-atom of —COOH of the functionalized MWCNTs. Fig. 5D displays the EFTEM of the nanocomposite material, representing the special distribution of FMWCNTs in the MOF-5 particles. The silicon impurity that is likely present in small amounts could also be linked to the MWCNTs during their synthesis process, which confirms the effective and homogeneous loading of the FMWCNTs in the nanocomposite.

During the growth of MOF-5 crystals, the FMWCNTs might have incorporated in the structure in a way that the polymeric structural units of MOF-5 get interrupted mainly by short length nanotubes during the aging of the crystals as seen in Fig. 5E and point analysis of EDX. The encircled regions in Fig. 5E show that the larger FMWCNTs are randomly clustered around the MOF-5 particles instead of being entrapped in the MOF-5 crystals. This difference can be attributed to the varying degree of functionalization of the MWCNTs, while the clustering behavior can be rendered to the hydrogen bonding interactions as discussed earlier from the FTIR spectra of these materials.

A simplified molecular structure of MOF-5@MWCNTs is depicted in Fig. 6. A plausible explanation of this nanocomposite structure can be understood in a way that MOF-5 attaches to the FMWCNTs by interacting with carboxylic groups, epoxy groups and the hydroxyl groups present on the FWCNTs surface. Recent studies have shown that the carboxyl functionalities on graphene oxide act as nucleation sites for the growth of MOF crystals and also affect the porosity (Jahan et al., 2010; Liu et al., 2013; Petit and Bandoz, 2015a, 2015b). The MWCNTs used in the present study were functionalized using acid treatment and therefore achieve a high number of carboxyl groups attached to the surface. In addition, there are some short length MWCNTs that contain more carboxyl functionalities than the high aspect ratio

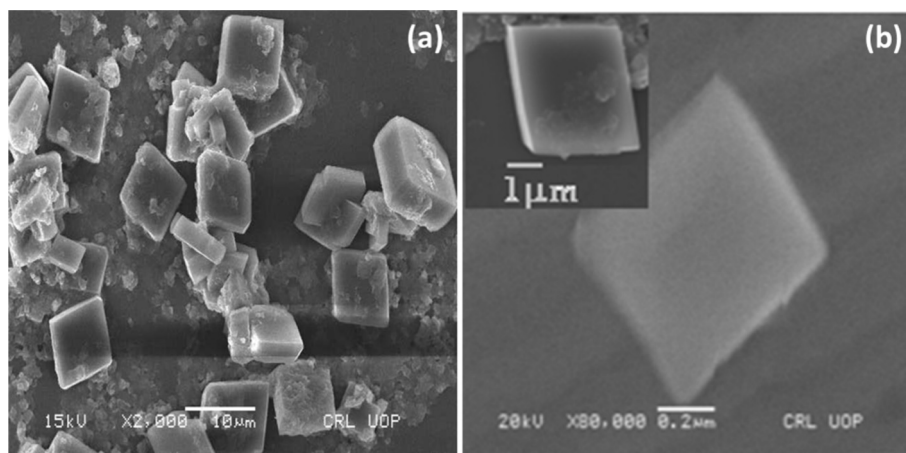


Fig. 4 SEM images of MOF-5.

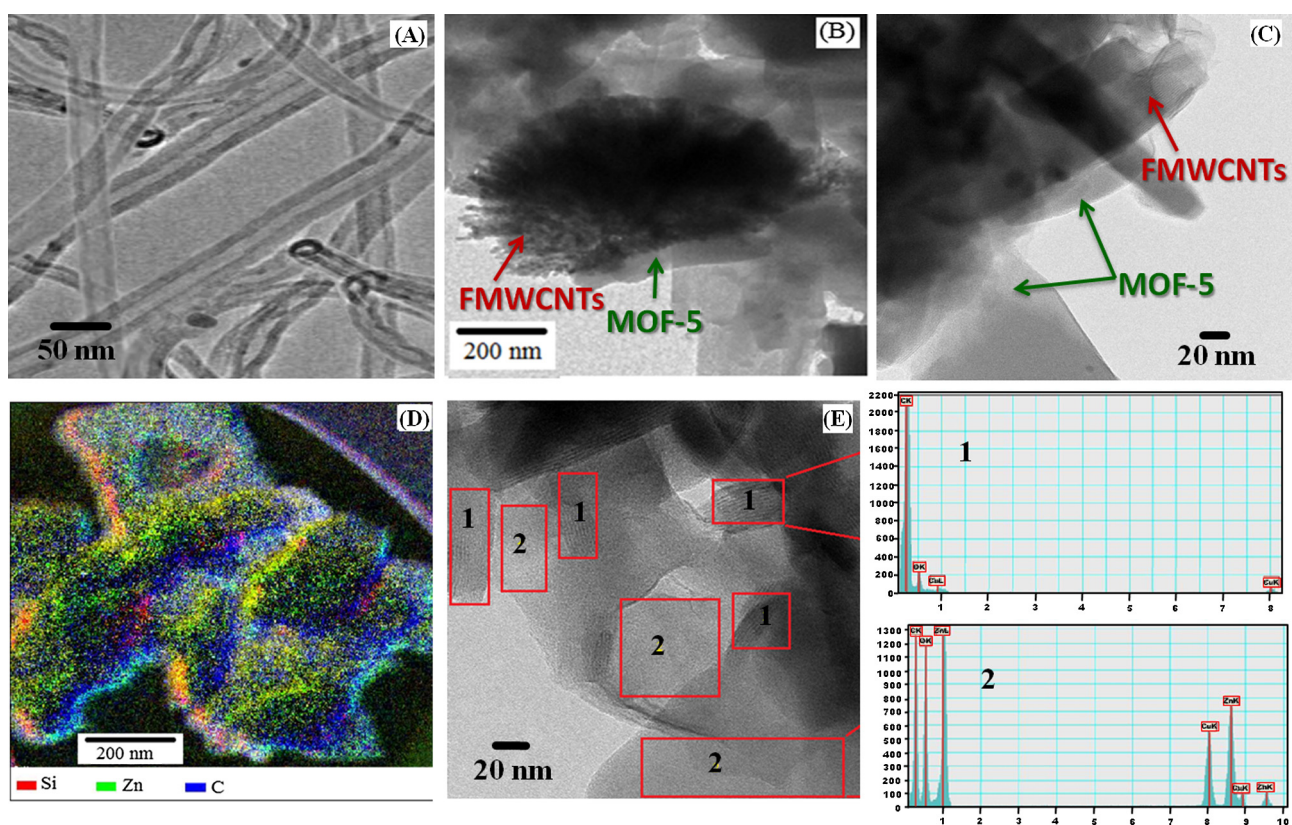


Fig. 5 TEM of (A) functionalized MWCNTs (B) and (C) MOF-5@FMWCNTs showing FMWCNTs clustering around MOF-5 particles (D) EFTEM of MOF-5@FMWCNTs and (E) HRTEM of FMWCNTs attached to MOF-5 particle with associated EDX.

MWCNTs. Both these types of functionalized MWCNTs seem to behave in a different manner in regard to their presence in the MOF-5 nanocomposite. MWCNTs with low aspect ratio are predominantly involved in providing the nucleation sites for the MOF-5 particles and forming intense hydrogen bonding than the peripheral MWCNTs with larger aspect ratio having no role in nucleation also supposed to be linked with hydrogen bonding with ZnO_4 tetrahedra of MOF-5, as shown in molecular model of the nanocomposite in Fig. 6 which suggest that the MOF-5 is surrounded by high aspect ratio

FMWCNTs network and provides peripheral stability to the nanocomposite, which can partially stabilize the MOF-5 nanocomposite upon exposure to ambient moisture conditions. The presence of low aspect ratio MWCNTs, anchoring the MOF-5 nanocomposite, imparts greater stability to the MOF, possibly involved in intermolecular hydrogen bonding with ZnO_4 tetrahedra.

MOF-5 synthesized by DEF approach in the current study displayed sufficiently high BET surface area and large pore volume. Table 1 summarizes the pore textural properties of

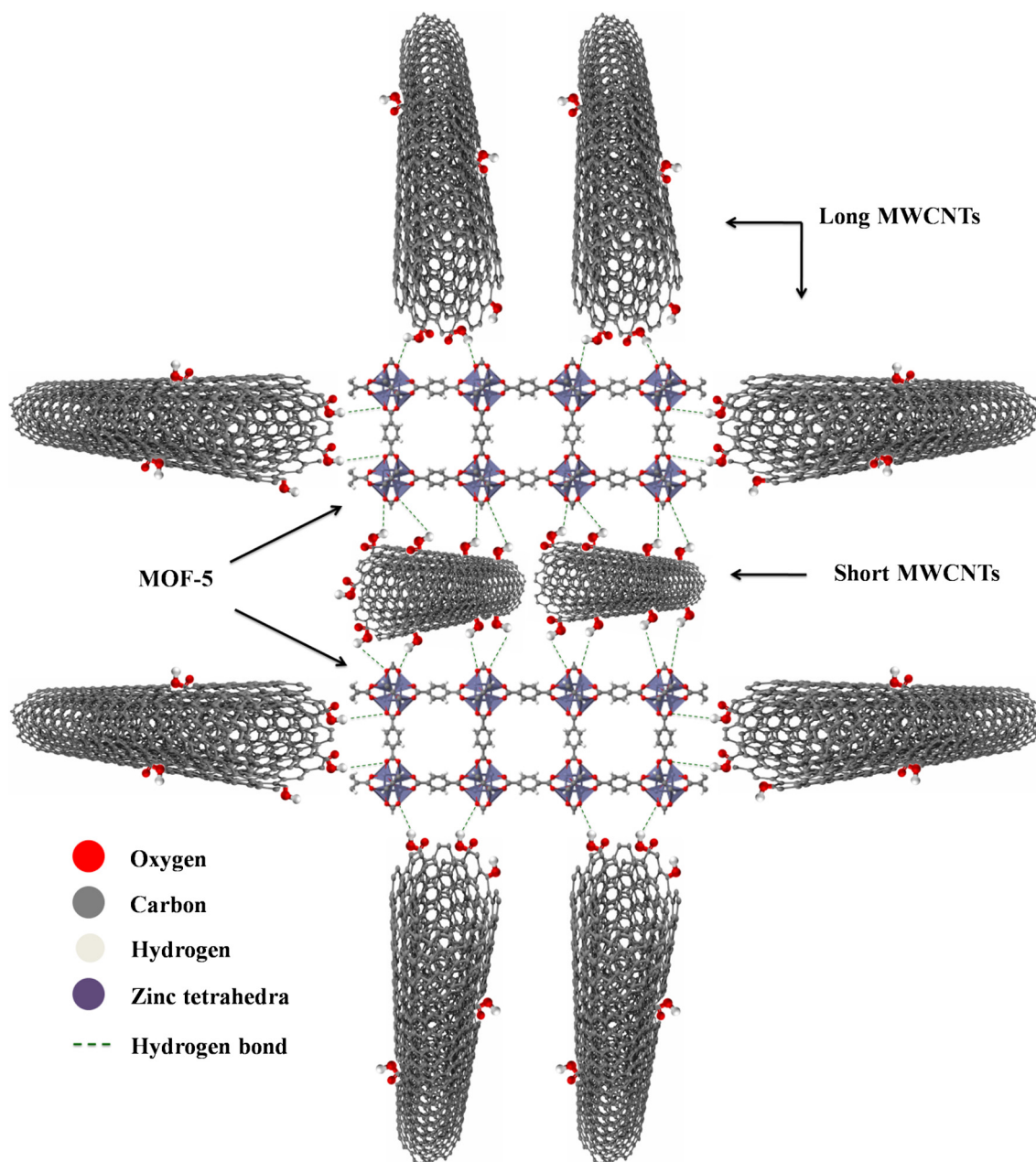


Fig. 6 Molecular model of MOF-5@FMWCNTs.

Table 1 Pore textural properties of MOF-5 and MOF-5@FMWCNTs.

No.	Sample	BET SSA ($\text{m}^2 \text{g}^{-1}$)	^a Pore volume ($\text{cm}^3 \text{g}^{-1}$)
1	MOF-5	713	0.48
2	MOF-5 (2 h)	121	0.07
3	MOF-5@FMWCNTs	728	0.50
4	MOF-5@FMWCNTs (1 week)	449	0.31

^a Pore volume calculated by DR method.

freshly prepared MOF-5, MOF-5 after 2 h exposed to ambient environment, freshly prepared MOF-5@FMWCNTs and MOF-5@FMWCNTs after 1 week exposure to an ambient environment at a relative humidity of 55% at 28 °C.

The BET surface area of the freshly prepared MOF-5 was $713 \text{ m}^2 \text{g}^{-1}$ that was reduced to $121 \text{ m}^2 \text{g}^{-1}$ after 2 h exposure to the ambient environment, due to the decomposition of the MOF-5 framework. After the formation of MOF-5@FMWCNTs nanocomposite, the surface area changed from $728 \text{ m}^2 \text{g}^{-1}$ to $449 \text{ m}^2 \text{g}^{-1}$ even after exposure to an ambient environment for 1-week. It is reasonable to attribute the extra stability of the nanocomposite to the attached FMWCNTs that were attached to the MOF-5 through hydrogen bonding and imparted their role in increasing the hydrostability of MOF-5.

4. Conclusion

The present study reveals that the microwave synthesis offers a good way to architect uniform sized cubic MOF-5 particles and MOF-5@FMWCNTs. The nanocomposite formed displays higher stability against atmospheric moisture due to the unique attachment of FMWCNTs. The hydrogen bonding interactions between ZnO₄ sub-unit of the MOF-5 framework and H-atom of the functionalized MWCNTs have been found to play a crucial role in stabilizing the MOF-5@FMWCNTs nanocomposite that has been confirmed by FTIR studies and supported by non-amorphization in XRD peaks of MOF-5@FMWCNTs. The experimental results reveal that the shorter MWCNTs containing a higher number of functionalities provide more nucleation sites for the MOF-5, while the longer MWCNTs provide peripheral stability to the MOF-5 nanocomposite structure. The hybrid MOF-5@FMWCNTs nanocomposite offers better adsorption capacity and retention of surface properties as compared to the high water sensitive bare MOF-5 framework, which can also be attributed to the intrinsic nature of the hydrophobic nature of MWCNTs.

References

- Bennett, T.D., Yue, Y., Li, P., Qiao, A., Tao, H., Greaves, N.G., Richards, T., Lampronti, G.I., Redfern, S.A.T., Blanc, F., Farha, O.K., Hupp, J.T., Cheetham, A.K., Keen, D.A., 2016. Melt-Quenched glasses of metal-organic frameworks. *J. Am. Chem. Soc.* 138, 3484–3492.
- Bordiga, S., Vitillo, J.G., Ricchiardi, G., Regli, L., Cocina, D., Zecchina, A., Arstad, B., Bjørgen, M., Hafizovic, J., Lillerud, K.P., 2005. Interaction of hydrogen with MOF-5. *J. Phys. Chem. B* 109, 18237–18242.
- Burtch, N.C., Jasuja, H., Walton, K.S., 2014. Water stability and adsorption in metal-organic frameworks. *Chem. Rev.* 114, 10575–10612.
- Chang, X., Henderson, W.M., Bouchard, D.C., 2015. Multiwalled carbon nanotube dispersion methods affect their aggregation, deposition, and biomarker response. *Environ. Sci. Technol.* 49, 6645–6653.
- Cui, Y., Li, B., He, H., Zhou, W., Chen, B., Qian, G., 2016. Metal-organic frameworks as platforms for functional materials. *Acc. Chem. Res.* 49, 483–493.
- Dai, W., Hu, J., Zhou, L., Li, S., Hu, X., Huang, H., 2013. Removal of dibenzothiophene with composite adsorbent MOF-5/Cu(I). *Energy Fuels* 27, 816–821.
- Ding, N., Li, H., Feng, X., Wang, Q., Wang, S., Ma, L., Zhou, J., Wang, B., 2016. Partitioning MOF-5 into confined and hydrophobic compartments for carbon capture under humid conditions. *J. Am. Chem. Soc.* 138, 10100–10103.
- Férey, G., Mellot-Draznieks, C., Serre, C., Millange, F., Dutour, J., Surblé, S., Margiolaki, I., 2005. A chromium terephthalate-based solid with unusually large pore volumes and surface area. *Science* 309, 2040–2042.
- Gadipelli, S., Guo, Z., 2014. Postsynthesis annealing of MOF-5 remarkably enhances the framework structural stability and CO₂ uptake. *Chem. Mater.* 26, 6333–6338.
- Gamage, N.D.H., McDonald, K.A., Matzger, A.J., 2016. MOF-5-polystyrene: direct production from monomer, improved hydrolytic stability, and unique guest adsorption. *Angew. Chem.* 128, 12278–12282.
- Greathouse, J.A., Allendorf, M.D., 2006. The interaction of water with MOF-5 simulated by molecular dynamics. *J. Am. Chem. Soc.* 128, 10678–10679.
- Hafizovic, J., Bjørgen, M., Olsbye, U., Dietzel, P.D., Bordiga, S., Prestipino, C., Lamberti, C., Lillerud, K.P., 2007. The inconsistency in adsorption properties and powder XRD data of MOF-5 is rationalized by framework interpenetration and the presence of organic and inorganic species in the nanocavities. *J. Am. Chem. Soc.* 129, 3612–3620.
- Han, J.T., Kim, S.Y., Woo, J.S., Lee, G.W., 2008. Transparent, conductive, and superhydrophobic films from stabilized carbon nanotube/silane sol mixture solution. *Adv. Mater.* 20, 3724–3727.
- Hu, M., Reboul, J., Furukawa, S., Torad, N.L., Ji, Q., Srinivasu, P., Ariga, K., Kitagawa, S., Yamauchi, Y., 2012. Direct carbonization of Al-based porous coordination polymer for synthesis of nanoporous carbon. *J. Am. Chem. Soc.* 134, 2864–2867.
- Huang, L., Wang, H., Chen, J., Wang, Z., Sun, J., Zhao, D., Yan, Y., 2003. Synthesis, morphology control, and properties of porous metal-organic coordination polymers. *Micropor. Mesopor. Mater.* 58, 105–114.
- Jahan, M., Bao, Q., Yang, J.X., Loh, K.P., 2010. Structure-directing role of graphene in the synthesis of metal-organic framework nanowire. *J. Am. Chem. Soc.* 132, 14487–14495.
- Kang, Z., Xue, M., Zhang, D., Fan, L., Pan, Y., Qiu, S., 2015. Hybrid metal-organic framework nanomaterials with enhanced carbon dioxide and methane adsorption enthalpy by incorporation of carbon nanotubes. *Inorg. Chem. Commun.* 58, 79–83.
- Kaye, S.S., Dailly, A., Yaghi, O.M., Long, J.R., 2007. Impact of preparation and handling on the hydrogen storage properties of Zn₄O(1,4-benzenedicarboxylate)₃ (MOF-5). *J. Am. Chem. Soc.* 129, 14176–14177.
- Khan, N.A., Jhung, S.H., 2009. Facile syntheses of metal-organic framework Cu-3 (BTC)₂(H₂O)₃ under ultrasound. *Bull. Kor. Chem. Soc.* 30, 2921–2926.
- Kim, J., Yeo, S., Jeon, J.-D., Kwak, S.-Y., 2015. Enhancement of hydrogen storage capacity and hydrostability of metal-organic frameworks (MOFs) with surface-loaded platinum nanoparticles and carbon black. *Micropor. Mesopor. Mater.* 202, 8–15.
- Kitagawa, S., Kitaura, R., Noro, S.I., 2004. Functional porous coordination polymers. *Angew. Chem. Int. Ed.* 43, 2334–2375.
- Li, H., Eddaoudi, M., O’Keeffe, M., Yaghi, O.M., 1999. Design and synthesis of an exceptionally stable and highly porous metal-organic framework. *Nature* 402, 276–279.
- Li, H., Shi, W., Zhao, K., Li, H., Bing, Y., Cheng, P., 2012. Enhanced hydrostability in Ni-doped MOF-5. *Inorg. Chem.* 51, 9200–9207.
- Liu, B., Shioyama, H., Akita, T., Xu, Q., 2008. Metal-organic framework as a template for porous carbon synthesis. *J. Am. Chem. Soc.* 130, 5390–5391.
- Liu, S., Sun, L., Xu, F., Zhang, J., Jiao, C., Li, F., 2013. Nanosized Cu-MOFs induced by graphene oxide and enhanced gas storage capacity. *Energy Environ. Sci.* 6, 818–823.
- Lu, C.M., Liu, J., Xiao, K., Harris, A.T., 2010. Microwave enhanced synthesis of MOF-5 and its CO₂ capture ability at moderate temperatures across multiple capture and release cycles. *Chem. Eng. J.* 156, 465–470.
- Lu, S.H., Ni Tun, M.H., Mei, Z.J., Chia, G.H., Lim, X., Sow, C.-H., 2009. Improved hydrophobicity of carbon nanotube arrays with micropatterning. *Langmuir* 25, 12806–12811.
- Mihaly, J.J., Zeller, M., Genna, D.T., 2016. Ion-directed synthesis of indium-derived 2,5-thiophenedicarboxylate metal-organic frameworks: tuning framework dimensionality. *Cryst. Growth Des.* 16, 1550–1558.
- Nguyen, J.G., Cohen, S.M., 2010. Moisture-resistant and superhydrophobic metal-organic frameworks obtained via postsynthetic modification. *J. Am. Chem. Soc.* 132, 4560–4561.
- Panella, B., Hirscher, M., 2005. Hydrogen physisorption in metal-organic porous crystals. *Adv. Mater.* 17, 538–541.
- Pasieka, J., Coulombe, S., Servio, P., 2014. The effect of hydrophilic and hydrophobic multi-wall carbon nanotubes on methane dissolution rates in water at three phase equilibrium (V–Lw–H) conditions. *Ind. Eng. Chem. Prod. Res.* 53, 14519–14525.
- Petit, C., Bandoz, T.J., 2015a. Engineering the surface of a new class of adsorbents: metal-organic framework/graphite oxide composites. *J. Colloid Interface Sci.* 447, 139–151.

- Petit, C., Bandoz, T.J., 2015b. MOF-graphite oxide composites: combining the uniqueness of graphene layers and metal-organic frameworks. *J. Colloid Interface Sci.* 447, 139–151.
- Petit, C., Burrell, J., Bandoz, T.J., 2011. The synthesis and characterization of copper-based metal-organic framework/graphite oxide composites. *Carbon* 49, 563–572.
- Rehman, A.U., Abbas, S.M., Ammad, H.M., Badshah, A., Ali, Z., Anjum, D.H., 2013. A facile and novel approach towards carboxylic acid functionalization of multiwalled carbon nanotubes and efficient water dispersion. *Mater. Lett.* 108, 253–256.
- Rosi, N.L., Eckert, J., Eddaoudi, M., Vodak, D.T., Kim, J., O’Keeffe, M., Yaghi, O.M., 2003. Hydrogen storage in microporous metal-organic frameworks. *Science* 300, 1127–1129.
- Rowsell, J.L., Yaghi, O.M., 2004. Metal-organic frameworks: a new class of porous materials. *Micropor. Mesopor. Mater.* 73, 3–14.
- Sabouni, R., Kazemian, H., Rohani, S., 2010. A novel combined manufacturing technique for rapid production of IRMOF-1 using ultrasound and microwave energies. *Chem. Eng. J.* 165, 966–973.
- Saha, D., Wei, Z., Deng, S., 2009. Hydrogen adsorption equilibrium and kinetics in metal-organic framework (MOF-5) synthesized with DEF approach. *Sep. Purif. Technol.* 64, 280–287.
- Sheikholeslam, M., Pritzker, M., Chen, P., 2012. Dispersion of multiwalled carbon nanotubes in water using ionic-complementary peptides. *Langmuir* 28, 12550–12556.
- Tang, J., Salunkhe, R.R., Liu, J., Torad, N.L., Imura, M., Furukawa, S., Yamauchi, Y., 2015. Thermal conversion of core-shell metal-organic frameworks: a new method for selectively functionalized nanoporous hybrid carbon. *J. Am. Chem. Soc.* 137, 1572–1580.
- Tang, J., Yamauchi, Y., 2016. Carbon materials: MOF morphologies in control. *Nat. Chem.* 8, 638–639.
- Torad, N.L., Hu, M., Kamachi, Y., Takai, K., Imura, M., Naito, M., Yamauchi, Y., 2013. Facile synthesis of nanoporous carbons with controlled particle sizes by direct carbonization of monodispersed ZIF-8 crystals. *Chem. Commun.* 49, 2521–2523.
- Tranchemontagne, D.J., Hunt, J.R., Yaghi, O.M., 2008. Room temperature synthesis of metal-organic frameworks: MOF-5, MOF-74, MOF-177, MOF-199, and IRMOF-0. *Tetrahedron* 64, 8553–8557.
- Tsao, C.-S., Yu, M.-S., Chung, T.-Y., Wu, H.-C., Wang, C.-Y., Chang, K.-S., Chen, H.-L., 2007. Characterization of pore structure in metal-organic framework by small-angle X-ray scattering. *J. Am. Chem. Soc.* 129, 15997–16004.
- Wang, R., Liu, X., Qi, D., Xu, Y., Zhang, L., Liu, X., Jiang, J., Dai, F., Xiao, X., Sun, D., 2015. A Zn metal-organic framework with high stability and sorption selectivity for CO₂. *Inorg. Chem.* 54, 10587–10592.
- Wei, X., Zheng, L., Luo, F., Lin, Z., Guo, L., Qiu, B., Chen, G., 2013. Fluorescence biosensor for the H₅N₁ antibody based on a metal-organic framework platform. *J. Mater. Chem. B* 1, 1812–1817.
- Yaghi, O.M., O’Keeffe, M., Ockwig, N.W., Chae, H.K., Eddaoudi, M., Kim, J., 2003. Reticular synthesis and the design of new materials. *Nature* 423, 705–714.
- Yang, C., Wang, D., Hu, X., Dai, C., Zhang, L., 2008. Preparation and characterization of multi-walled carbon nanotube (MWCNTs)-supported Pt-Ru catalyst for methanol electrooxidation. *J. Alloys Compd.* 448, 109–115.
- Yang, J.M., Liu, Q., Sun, W.Y., 2014. Co(II)-doped MOF-5 nano/microcrystals: solvatochromic behaviour, sensing solvent molecules and gas sorption property. *J. Solid State Chem.* 218, 50–55.
- Yang, S.J., Choi, J.Y., Chae, H.K., Cho, J.H., Nahm, K.S., Park, C. R., 2009. Preparation and enhanced hydrostability and hydrogen storage capacity of CNT@ MOF-5 hybrid composite. *Chem. Mater.* 21, 1893–1897.
- Yue, Y., Fulvio, P.F., Dai, S., 2015a. Hierarchical Metal-organic framework hybrids: Perturbation-assisted nanofusion synthesis. *Acc. Chem. Res.* 48, 3044–3052.
- Yue, Y., Rabone, J.A., Liu, H., Mahurin, S.M., Li, M.R., Wang, H., Lu, Z., Chen, B., Wang, J., Fang, Y., Dai, S., 2015b. A flexible metal-organic framework: guest molecules controlled dynamic gas adsorption. *J. Phys. Chem. C* 119, 9442–9449.
- Zhang, W., Hu, Y., Ge, J., Jiang, H.L., Yu, S.H., 2014. A facile and general coating approach to moisture/water-resistant metal-organic frameworks with intact porosity. *J. Am. Chem. Soc.* 136, 16978–16981.
- Zhang, Z., Nguyen, H.T.H., Miller, S.A., Ploskonka, A.M., DeCoste, J.B., Cohen, S.M., 2016. Polymer-metal-organic frameworks (polyMOFs) as water tolerant materials for selective carbon dioxide separations. *J. Am. Chem. Soc.* 138, 920–925.
- Zhao, Y., Li, X., Liu, J., Wang, C., Zhao, Y., Yue, G., 2016. MOF-derived ZnO/Ni₃ZnC_{0.7}/C hybrids yolk-shell microspheres with excellent electrochemical performances for lithium ion batteries. *ACS Appl. Mater. Interfaces* 8, 6472–6480.
- Zhao, Z., Li, Z., Lin, Y., 2009. Adsorption and diffusion of carbon dioxide on metal-organic framework (MOF-5). *Ind. Eng. Chem. Res.* 48, 10015–10020.
- Zou, G., Jia, X., Huang, Z., Li, S., Liao, H., Hou, H., Huang, L., Ji, X., 2016. Cube-shaped porous carbon derived from MOF-5 as advanced material for sodium-ion batteries. *Electrochim. Acta* 196, 413–421.